



# Study on surface subsidence prediction method of shallow coal seam backfill-strip mining under the hard roof

Huaizhi Bo<sup>1,2</sup> · Guangli Guo<sup>3,4</sup> · Huaizhan Li<sup>3,4</sup> · Yuezong Wang<sup>1,2</sup> · Qian Jiang<sup>3,4</sup> · Shaohao Hu<sup>1,2</sup> · Fanglong Zhang<sup>1,2</sup>

Received: 24 September 2022 / Accepted: 3 June 2023 / Published online: 29 June 2023  
© Springer-Verlag GmbH Germany, part of Springer Nature 2023

## Abstract

Because of the easily caused damage to ground buildings by shallow coal seam mining under the hard roof, backfill-strip mining has been gradually adopted to realize the sustainable development of mining and protection of ground buildings. The surface subsidence prediction method in backfill-strip mining is not clear enough to the shallow coal seam under the hard roof. This paper adopts the numerical simulation method to study the surface movement characteristics of shallow coal seam backfill-strip mining under the hard roof. The results show that the maximum surface subsidence and the stress of the filling body are directly proportional to the width of the caving mining working face in the range of 30~80 m. The stress of the coal pillars on both sides is unchanged. The thickness from the wave band to the surface conforms to the quadratic function. The characteristics of surface movement conform to the prediction model of the probability integral method. Based on the probability integral method, the superposition calculation method of backfill-strip mining is deduced, and the prediction parameters calculation equation of the whole backfill-strip mining area is given. Finally, 5 backfill-strip mining schemes are designed in combination with the case. According to the protection index and the economic benefits, the best mining scheme is determined. The research results provide a reference for surface subsidence prediction in similar geological conditions.

**Keywords** Shallow coal seam mining · Hard roof · Backfill-strip mining · Numerical simulation · Subsidence prediction

## Introduction

China is one of the largest coal mining countries in the world. Subsidence caused by underground coal mining has damaged buildings and arisen a series of environmental

problems (Saeidi et al. 2012; Nie et al. 2013; Salmi et al. 2017; Diao et al. 2019; Guo et al. 2019; Venvik et al. 2020). Therefore, reasonable prediction of subsidence is an effective means to protect the buildings (Li et al. 2019; Guo et al. 2020; Vusovic et al. 2021; Khanal and Hodgkinson 2021). The traditional surface subsidence prediction method is suitable for most mining modes (Zhu et al. 2016; Ghabraie et al. 2017; Yuan et al. 2020; Wei et al. 2022; Jiang et al. 2022). However, shallow coal seam mining under a hard roof will cause sudden roof breaking and dynamic disasters such as rock bursts and large area weighting when the hanging roof area is too large (Tan et al. 2011; He et al. 2012, 2016; Wang et al. 2015a, b; Zhou et al. 2019), resulting in surface subsidence pits and other discontinuous damage. The buildings are seriously damaged, and the characteristics of surface subsidence are not consistent with the traditional mining subsidence theory.

To alleviate the mine pressure and subsidence, many scholars have done a lot of research (Wang and Miao 2009; Senol 2012; Goodarzi and Salimi 2015; Khajeh et al. 2020; Wang et al. 2020; Shirmohammadi et al. 2021; Jahandari et al. 2022; Khajeh et al. 2021; Khaksar Najafi et al. 2021;

✉ Yuezong Wang  
2289346115@qq.com  
Huaizhi Bo  
bohuaizhi@163.com

<sup>1</sup> Shandong Provincial Lunan Geology and Exploration Institute, Jining 272000, Shandong, China

<sup>2</sup> Technology Innovation Center of Restoration and Reclamation in Mining Induced Subsidence Land, Ministry of Natural Resources, Jining 272000, Shandong, China

<sup>3</sup> School of Environment Science and Spatial Informatics, China University of Mining and Technology, Xuzhou 221116, Jiangsu, China

<sup>4</sup> NASG Key Laboratory of Land Environment and Disaster Monitoring, China University of Mining and Technology, Xuzhou 221116, Jiangsu, China

Khajeh et al. 2022; Ngamkhanong et al. 2022). From the analysis of mining methods, backfill mining and strip mining are mostly adopted (Zha et al. 2011; Xuan and Xu 2014; Zhang et al. 2015; Li et al. 2019a, b). However, the backfill mining cost is high and strip mining has a low recovery ratio. Therefore, backfill-strip mining is adopted to control subsidence and protect buildings. The backfill-strip mining divides the mining face into several strip working faces. Firstly, backfill mining is carried out according to the way of filling one strip and leaving one strip. After the backfill bodies achieve a certain bearing capacity, the coal pillars between the backfill working faces are recycled (Guo et al. 2023). Finally, the two adjacent working faces are strip mining face and backfill mining face, as shown in Fig. 1.

The backfill-strip mining is gradually applied to shallow coal seam mining for buildings protection because of its good effect, high resource recovery rate, and low filling cost (Guo et al. 2004; Wang et al. 2015a, b; Li et al. 2016; Zhu et al. 2019a, b). The traditional subsidence prediction method in backfill-strip mining is to divide the mining area into several small working faces of caving mining and backfill mining and predict these small working faces respectively. Finally, the subsidence value of each small working face is superimposed in space to obtain the surface subsidence value of backfill-strip mining (Zhang et al. 2017; Dong et al. 2018). However, the insufficient mining of each small working face makes it difficult to set prediction parameters, resulting in low prediction accuracy. Zhu et al. (2019a, b, 2021) proposed a new backfill-strip mining prediction method. The backfill-strip mining area was set as upper and lower layers from the vertical angle, and the predicted parameters of each layer were given. This method is reasonable, simple, and accurate.

Based on the above methods, a coal mine in Shanxi Province, China, which has a shallow coal seam under the hard roof, is chosen as the engineering background to study the surface movement and deformation characteristics of backfill-strip mining by numerical simulation and deduce the backfill-strip

mining superposition calculation method based on the probability integral theory. Taking the mining area as a whole, the calculation formula of prediction parameters of backfill-strip mining is given. Finally, 5 backfill-strip mining schemes are designed and subsidence prediction is evaluated based on the case study. Research results provide a reference for subsidence prediction of similar geological and mining conditions.

## Overview of the study area

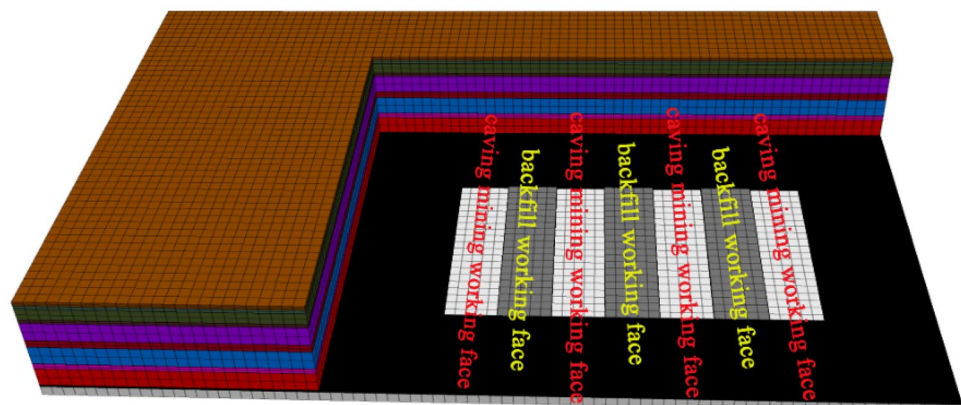
The study area is located in Datong City, Shanxi Province in China. The mining No. 3 coal seam is chosen as the simulation study area. The average thickness, mining depth, and dip angle of the No. 3 coal seam are 2 m, 100 m, and 3°, respectively, which is considered to be the horizontal coal seam. The No. 3 coal seam is hosted in the Datong Formation of the Middle Jurassic, the thickness of this formation is 176 m, mainly consisting of gray, gray-brown mudstone, gray, gray-white sandstone, and coal seam. The strata above the Datong Formation is the Yungang Formation with a thickness of 104 m, which consists of gray silty sandstone, gray sandstone, and conglomerate rock. Above the stratum is the Quaternary which is a thin layer of only 4 m. The roof of the study area is fine, dense, and hard sandstone with a thickness of 20 m. Detailed information on strata is presented in the numerical simulation.

## Study of the numerical simulation experiment

### Establishment of the numerical model

To analyze the surface movement and deformation characteristics of shallow coal seam backfill-strip mining under

**Fig. 1** Schematic diagram of backfill-strip mining



First: backfill mining second: caving mining

the hard roof, FLAC3D numerical simulation software was used to establish the numerical model of the whole strata with the drilling data in the study area. The size of the model is 800 m × 500 m × 110 m. The length and width of each unit are fixed at 10 m and the height varies with the rock strata thickness. The left and right boundaries of the model are fixed in the *x*-direction, the front and rear boundaries are fixed in the *y*-direction, the lower boundary is fixed in the *z*-direction, and the top is free. The numerical model is shown in Fig. 2.

The rock layers of the model are siltstone, coal, fine sandstone, conglomerate, coarse sandstone, conglomerate, coarse sandstone, fine sandstone, coarse sandstone, fine sandstone, fine sandstone, and the thickness is 10 m, 2 m, 20 m, 6 m, 20 m, 8 m, 20 m, 4 m, 12 m, 4 m, and 4 m, respectively. The loose layer occurs from bottom to top. The constitutive model of each element in FLAC3D is Mohr–Coulomb. When calibrating the parameters of the FLAC3D model, several caving mining tests with different rock mechanical parameters are repeatedly performed until the subsidence coefficient *q*, which is calculated as the ratio of maximum surface subsidence to mining height, is similar to actual subsidence coefficient in mining area. The distribution and simulation mechanical parameters of each stratum in the mining area are shown in Table 1.

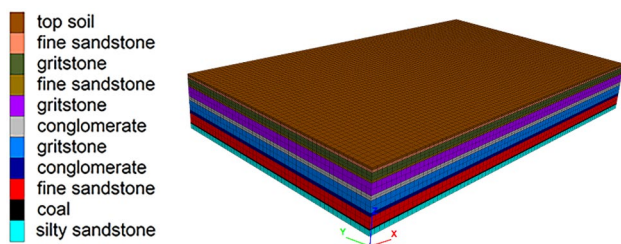


Fig. 2 Numerical model of backfill-strip mining

### Simulation scheme

- (1) The model is to simulate the influence of different widths of the caving mining working face in backfill-strip mining on surface movement and deformation and bearing stress of the filling body. The filling rate is 80%, and the backfill working face width is 40 m. The specific scheme is shown in Table 2. The excavation and filling are completed in the FLAC3D model. After the model is balanced, the data is generated by the FISH language built into the software to analyze the bearing stress of the filling body and the surface movement and deformation.
- (2) The experiment simulates the characteristics of surface movement and deformation under the different filling rates. The stiffness of the filling body is varied with the elastic modulus, based on which the filling rates are adjusted. The width of the caving mining working face and backfill working face is set to 40 m, to analyze the influence of different filling rates on surface movement and deformation. The specific scheme is shown in Table 3.

### Analysis of simulation results

- (1) Distribution characteristics of surface subsidence with different widths of the caving mining working face.

The surface subsidence values of different widths of the caving mining working face are generated from the model along the main section, and the variation characteristics of surface subsidence with the width values are plotted, as shown in Fig. 3. The maximum surface subsidence value of each scheme is calculated, and the relationship between

Table 1 Simulation mechanical parameters of the mining area

Rock stratum	Thickness (m)	Bulk modulus (GPa)	Shear modulus (GPa)	Cohesion (MPa)	Tensile strength (MPa)	Internal friction angle (°)	Density (kg/m <sup>3</sup> )
Topsoil	4	0.25	0.16	0.10	0.05	15	1200
Fine sandstone	4	1.37	0.94	0.90	0.75	30	2400
Gritstone	12	1.07	0.74	0.80	0.65	30	2300
Fine sandstone	4	1.37	0.94	0.90	0.75	30	2400
Gritstone	20	0.96	0.61	0.70	0.60	30	2300
Conglomerate	8	1.15	0.73	0.80	0.70	28	2100
Gritstone	20	0.96	0.61	0.70	0.60	30	2300
Conglomerate	6	1.03	0.65	0.75	0.60	28	2100
Fine sandstone	20	1.56	1.16	1.20	0.90	35	2500
Coal	2	0.67	0.40	0.60	0.50	25	1800
Silty sandstone	10	5.00	4.00	4.00	3.50	35	2400

**Table 2** Scheme design of different widths of the caving mining working face

Scheme	1	2	3	4	5	6
Filling rate (%)	80	80	80	80	80	80
Length of the backfill working face (m)	40	40	40	40	40	40
Length of the caving mining working face (m)	30	40	50	60	70	80

**Table 3** Scheme design of different filling rates

Scheme	1	2	3	4
Filling rate (%)	70	75	80	85
Length of the backfill working face (m)	40	40	40	40
Length of the caving mining working face (m)	40	40	40	40

the maximum surface subsidence and the width of the caving mining working face is analyzed, as shown in Fig. 4. It can be seen that within the scope of the study, the surface subsidence value increases with the increase of the width of the caving mining working face. The surface subsidence curve is continuous and gentle, and there is no wavy subsidence. When the width of the caving mining working face increases from 30 to 80 m, the maximum surface subsidence value increases from 365 to 732 mm. The maximum subsidence value, which increases linearly with the increase of the width of the caving mining working face, can be calculated by Eq. (1):

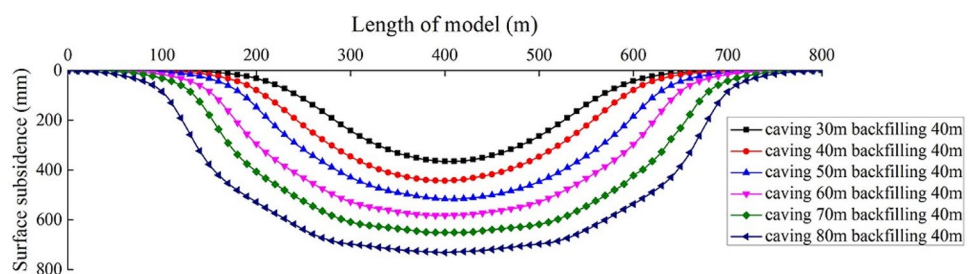
$$y = 7.2077x + 152.013 \tag{1}$$

The correlation coefficient is 0.9990.

(2) Analysis of development height of the wave band with different widths of the caving mining working face.

To analyze the development height of the wave band with different widths of the caving mining working face, the highest development position of the wave band in different mining schemes is generated along the main section,

**Fig. 3** Surface subsidence distribution curves of different widths of the caving mining working face



and the distance to the surface is calculated. The variation curve of the distance and the width is calculated, as shown in Fig. 5. Because only the data at the model node can be extracted, the development height of the wave band in the model is smaller than the extracted data. When the width of the caving surface is 30 m, the development height of the wave band is small, and the maximum height is less than 20 m above the coal seam, which is located inside the hard roof. At this point, only the part of the hard roof has wavy bending subsidence, and the maximum position is about 78 m under the surface. When the width of the caving mining working face increases to 40 m, the height of the wave band remains unchanged, which is due to the strength and stiffness of the hard roof being larger, resulting in the wave band do not break through the hard roof and upward development. As the width of the caving mining working face continues to increase, the wave band development height will exceed the thickness of the hard

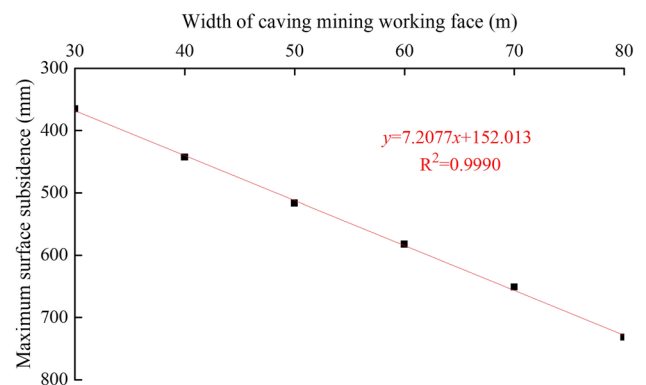


**Fig. 4** Variation relationship of maximum surface subsidence with the width of caving mining working face



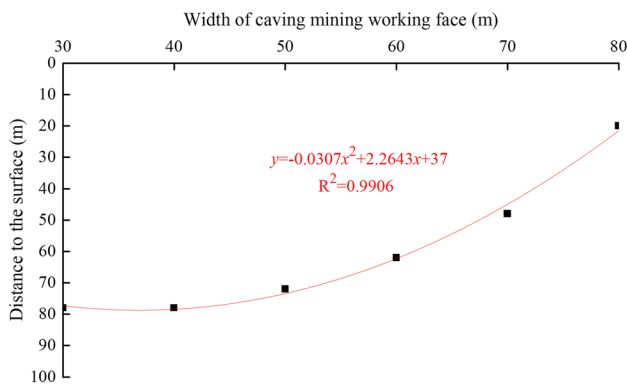


**Fig. 5** Variation relationship of development height of the wave band with the width of the caving mining working face

roof and gradually develops upward. When the width of the caving mining working face increases to 80 m, the highest point of the wave band is 20 m away from the surface. The distance from the highest position of the wave band to the surface can be calculated by Eq. (2):

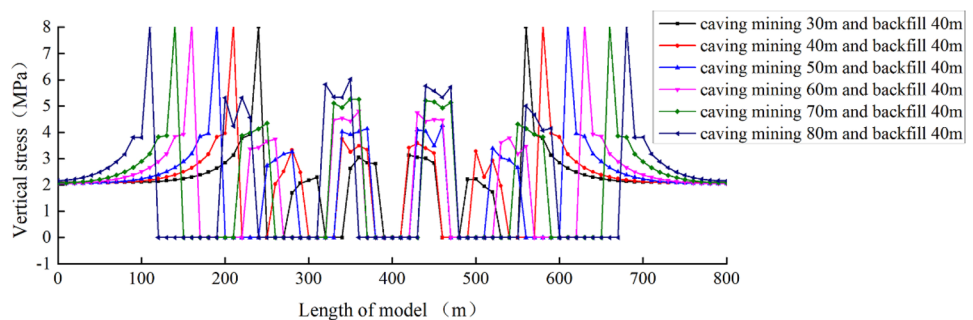
$$y = 0.0307x^2 + 2.2643x + 37 \tag{2}$$

The correlation coefficient is 0.9906.

(3) Distribution characteristics of bearing stress of coal pillars and filling bodies with different widths of the caving mining working face.

With the increase of the width of the caving mining working face in backfill-strip mining under the hard roof, the hanging roof area increases accordingly, which will concentrate the stress of coal pillars and filling bodies. When the filling body bearing stress exceeds its maximum value, it will be destroyed. In severe cases, the hard roof will be unstable, resulting in discontinuous subsidence on the surface. To analyze the various characteristics of bearing stress of coal pillars and filling bodies with different widths of the caving mining working face, the vertical stress was extracted from the model along the horizontal direction of the coal seam. The variation curves of bearing

**Fig. 6** Variation curves of stress of coal pillars and filling bodies with different widths of the caving surface



stress of coal pillars and filling bodies are calculated, as shown in Fig. 6. As the caving mining working face is mined, the initial bearing stress is transferred to the filling body and coal pillars on both sides, increasing the stress of the coal pillars and the filling body. The filling body is gradually compacted, and the stress is transferred largely from the roof to the coal pillars on both sides, resulting in larger bearing stress of coal pillars than the filling body. Although backfill-strip mining is adopted, the hard roof can still be regarded as the bending deformation of the fixed beam. Due to the cantilever effect of the hard roof, the bearing stress near the coal pillars on both sides is smaller than that in the middle. The analysis of the bearing stress of a single filling body shows that the bearing stress at both ends of filling bodies is larger than that in the middle with the increase of the width of the caving mining working face. This is because the stress of the caving mining working face is transferred to the two adjacent filling surfaces. The larger the hanging roof area of the goaf, the greater the bearing stress at both ends of the filling body. At this point, the filling bodies on both sides of the goaf are considered coal pillars for the local area. Figure 7 shows the relationship between the extreme value of stress of coal pillars and filling bodies and the width of the caving mining working face. With the increase of the width of the caving mining working face, the extreme value of the coal pillar stress is basically stable at about 8 MPa. The extreme value of the stress of the filling body increases linearly with the increase of the width of the caving mining working face. The relationship is shown in Eq. (3):

$$y = 0.0582x + 1.2910 \tag{3}$$

The correlation coefficient is 0.9950.

According to the relationship between the bearing stress of the filling body and the width of the caving mining working face, in actual mining, the width of the caving mining working face can be designed according to the allowable stress value of the filling body to ensure the stability of the filling body.

(4) Surface movement and deformation characteristics of different filling rates.

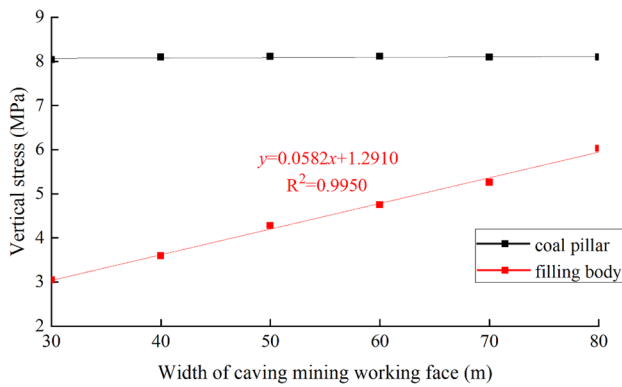


**Fig. 7** Variation relationship between the bearing stress of coal pillars and filling bodies and the width of the caving mining working face

To analyze the surface movement and deformation characteristics of different filling rates, the width of the caving mining working face and the width of the backfill working face are all set to 40 m, and four schemes with filling rates of 70%, 75%, 80%, and 85%, respectively, are simulated. The surface subsidence and horizontal movement data of four schemes are extracted, and the surface tilt and horizontal deformation are calculated. The surface movement and deformation curves of four schemes are drawn, as shown in Fig. 8. The surface movement and deformation characteristics of the four schemes meet the general law of mining, which conforms to the probability integral method prediction model (Wang and Deng 2012; Wang and Guo 2020).

To accurately predict the surface movement and deformation in backfill-strip mining, it is necessary to determine the prediction parameters of the probability integral method. From the analysis of subsidence space, the goaf is divided into upper and lower parts by the horizontal line where the filling body is compacted. The surface subsidence of the backfill-strip mining can be regarded as the result of the combined effect of the caving mining in the upper part and the strip mining in the lower part. Three schemes of the backfill-strip mining (filling rate is 80%, the width of the caving mining working face and backfill working face is 40 m), the caving mining (the mining thickness is 0.4 m), and the strip mining (the mining thickness is 1.6 m, the mining width and remaining width are 40 m) are simulated respectively. The surface subsidence curve is drawn by analyzing the relationship among them, as shown in Fig. 9. It can be seen from the diagram that the sum of the subsidence values of the caving mining and the strip mining is equal to the subsidence value of the backfill-strip mining. The maximum subsidence value is a 31-mm difference and the error is 7%, which meets the industrial requirements.

Therefore, this method can be used to predict the subsidence of the backfill-strip mining, and the theoretical

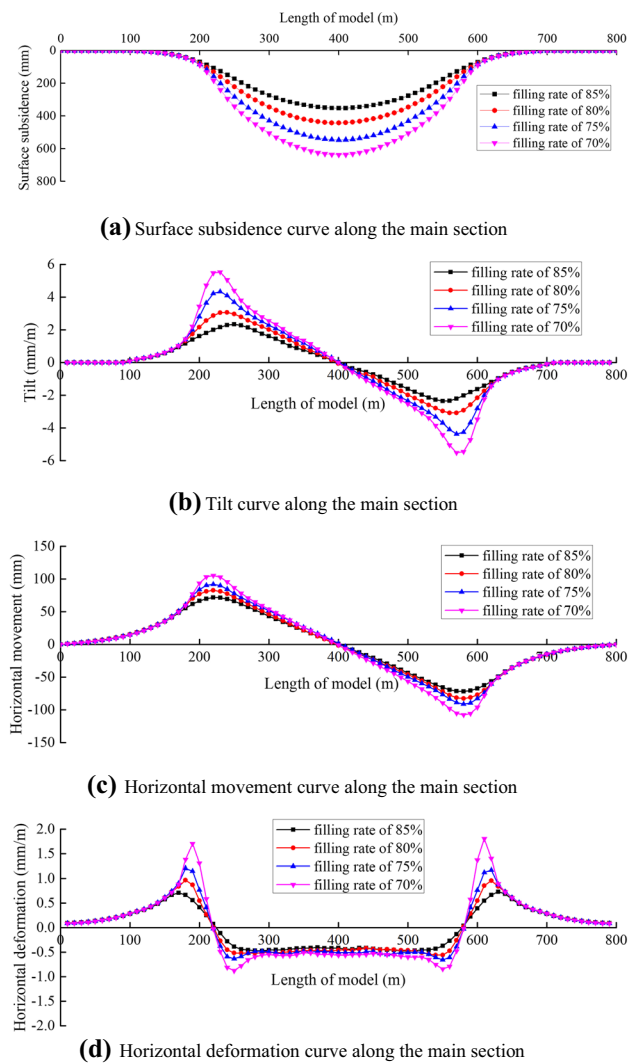


**Fig. 8** Surface movement and deformation curve of different filling rates

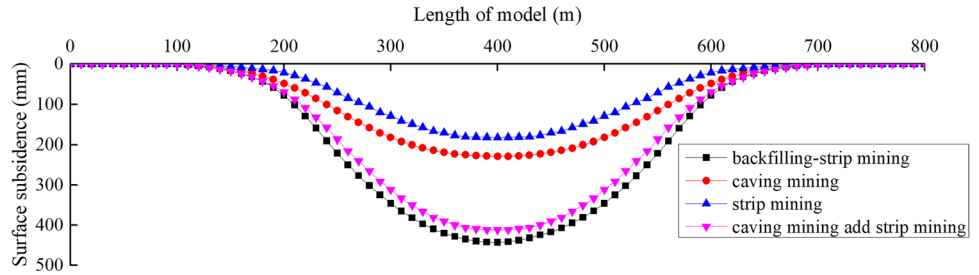
calculation equation of the predicted parameters of the probability integral method is introduced in detail below.

## Prediction method of surface subsidence

### Introduction of probability integral method

The probability integral method is based on the stochastic medium theory. The theoretical model holds that the medium is composed of medium particles similar to sand or relatively small rock blocks. The particles completely lose contact and can move relatively, as shown in Fig. 10. It is assumed that these medium particles are some small balls of the same size

**Fig. 9** Comparison diagram of surface subsidence of different mining methods



and uniform mass, and are arranged in a uniform square with the same size. When a ball in a square is removed, one of the two adjacent balls in the upper layer will fall and fill the square due to gravity. It is assumed that two adjacent balls in the upper layer of the square fall into the square completely randomly and with the same probability, and so on. Then, the probability distribution diagram of particle movement can be obtained by recording the probability of each square grid due to the release of a small ball in the  $a_1$  grid, as shown in Fig. 10(b). If the size of the grid is very small, the histogram tends to be a density curve with a normal distribution (Deng et al. 2014).

According to the above reasoning, the mathematical model of probability integral method can be expressed as follows:

The surface subsidence value at any point A (x, y) is shown in Eq. (4):

$$W(x, y)_A = W_0 C(x) C(y) \tag{4}$$

$$\begin{cases} W_0 = mq\cos\alpha \\ C(x) = \frac{1}{\sqrt{\pi}} \left[ \int_{-\sqrt{\pi}\frac{x}{r}}^0 e^{-\lambda^2} d\lambda + \int_0^{\sqrt{\pi}\frac{L-x}{r}} e^{-\lambda^2} d\lambda \right] \\ C(y) = \frac{1}{\sqrt{\pi}} \left[ \int_{-\sqrt{\pi}\frac{y}{r_1}}^0 e^{-\lambda^2} d\lambda + \int_0^{\sqrt{\pi}\frac{L-y}{r_2}} e^{-\lambda^2} d\lambda \right] \end{cases} \tag{5}$$

where  $W_0$  is the surface maximum subsidence value of full mining;  $m$  is thickness of coal seam;  $q$  is surface subsidence coefficient;  $\alpha$  is dip angle of coal seam;  $C(x)$  and  $C(y)$  are subsidence distribution coefficient of the point A (x, y) in strike and dip main section;  $l$  and  $L$  are calculation mining width along the strike and dip direction after considering the inflection point offset;  $r$  is major influence radius of the strike direction;  $r_1$  and  $r_2$  are major influence radius of the dip direction, where  $r_1$  is the downhill direction and  $r_2$  is the uphill direction.

**Superposition calculation method in the backfill-strip mining**

Through the above analysis, it is determined that the surface movement and deformation characteristics of shallow coal seam backfill-strip mining under the hard roof meet the general mining law. According to a large number of engineering practices and theoretical analyses, the characteristics of surface movement and deformation can be predicted by the probability integral method prediction model. Surface movement and deformation of the backfill-strip mining are calculated based on the probability integral method mathematical model.

The surface subsidence caused by the backfill-strip mining can be considered to be caused by the combined effect of the caving mining of upper coal seams and the strip mining of lower coal seams. Taking Fig. 11 as an example, the total thickness of the coal seam is  $m$ . It is

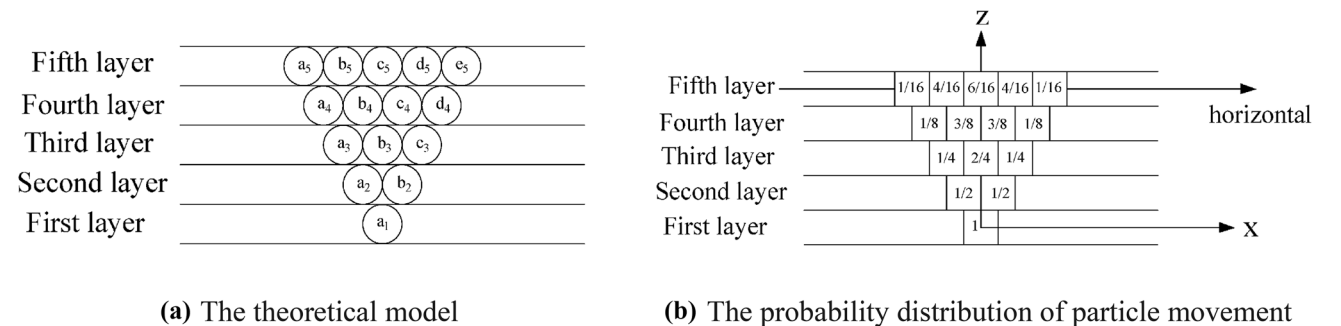


**Fig. 10** The theoretical model of granular medium as random medium

assumed that the height of the filling body after compaction is  $m_2$ , and the equivalent mining height is  $m_1$ . The equivalent mining height refers to the difference between the actual mining height and the height of fully compacted filling body (Miao et al. 2010). The calculation equation is  $m_1 = (1 - \rho)m$ .  $\rho$  is the design filling rate of the working face. The surface subsidence can be regarded as the combined effect of the coal seam where  $m_1$  is mined by the caving mining and the coal seam where  $m_2$  is mined by the strip mining. The surface movement and deformation of the backfill-strip mining are obtained by superposition calculation of the two parts.

$$\begin{cases} m_1 = (1 - \rho)m \\ m_2 = \rho m \end{cases} \quad (6)$$

The subsidence coefficient of strip mining is related to mining width and retaining width. The empirical calculation equation is as follows:

$$q_t/q = 0.2663e^{-0.5753m} \cdot \lambda^{2.6887} \cdot \ln\left(\frac{bH}{a}\right) + 0.0336 \quad (7)$$

where  $q_t$  is the subsidence coefficient of the strip mining;  $q$  is the subsidence coefficient of the caving mining;  $a$  is the width of the backfill working face;  $b$  is the width of the caving mining working face;  $\lambda$  is the recovery rate of the strip mining,  $\lambda = \frac{b}{a+b}$ ;  $H$  is the mining depth of coal seam.

Therefore, the surface subsidence ( $W_1$ ) caused by the caving mining of the upper coal seams and the surface subsidence ( $W_2$ ) caused by the strip mining of the lower coal seams can be calculated as shown in Eq. (8):

$$\begin{cases} W_1 = m_1 q \cos \alpha = (1 - \rho) m q \cos \alpha \\ W_2 = m_2 q_t \cos \alpha = \rho m q \left[ 0.2663 e^{-0.5753m} \cdot \lambda^{2.6887} \cdot \ln\left(\frac{bH}{a}\right) + 0.0336 \right] \cos \alpha \end{cases} \quad (8)$$

where  $\alpha$  is the dip angle of the coal seam.

According to Eq. (8), the subsidence coefficient ( $q_d$ ) of the backfill-strip mining can be obtained:

$$q_d = \frac{W_1 + W_2}{m \cos \alpha} = \left\{ \rho \cdot \left[ 0.2663 e^{-0.5753m} \cdot \lambda^{2.6887} \cdot \ln\left(\frac{bH}{a}\right) + 0.0336 \right] + 1 - \rho \right\} \cdot q \quad (9)$$

The other subsidence prediction parameters of the probability integral method can be selected according to the prediction parameters of the strip mining. The empirical calculation equation is as follows:

Tangent of major influence angle ( $\tan \beta_d$ ) of the backfill-strip mining:

$$\tan \beta_d = (1.076 - 0.0014H) \cdot \tan \beta \quad (10)$$

where  $\tan \beta$  is the tangent of major influence angle in the caving mining.

Horizontal movement coefficient ( $b_d$ ) of the backfill-strip mining:

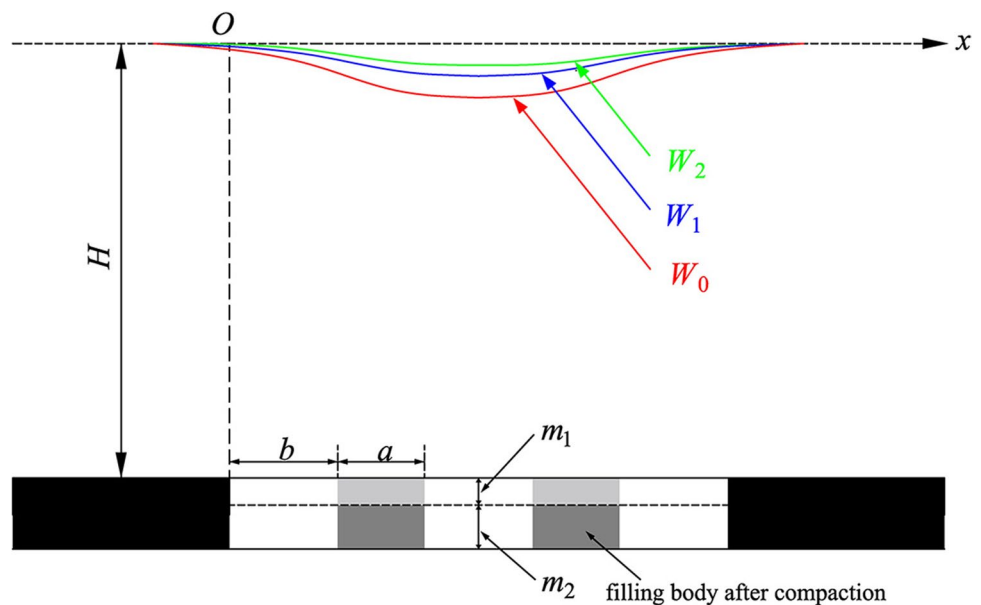
$$b_d = \left[ -0.0002 \frac{H(a+b)}{b} + 0.8786 \right] \cdot b_0 \quad (11)$$

where  $b_0$  is the horizontal movement coefficient in the caving mining.

Inflection point offset ( $S_d$ ) of the backfill-strip mining:

$$S_d = 0.0673 \frac{b^2 H}{a(a+b)} + 2.564 \quad (12)$$

Fig. 11 Schematic diagram of superimposed calculation in the backfill-strip mining





From a security point of view, the inflection point offset is generally taken as 0.

Propagation angle of extraction ( $\theta_d$ ) of the backfill-strip mining:

$$\theta_d = \theta_0 \tag{13}$$

where  $\theta_0$  is the propagation angle of extraction in the caving mining.

The subsidence coefficient ( $q$ ), the horizontal movement coefficient ( $b_0$ ), the tangent of major influence angle ( $\tan\beta$ ), the inflection point offset ( $S$ ), and the propagation angle of extraction ( $\theta_0$ ) in the above equation can be comprehensively determined according to geological and mining conditions and measured data.

### Case application

There are many buildings in the study area and the underground coal mining is highly active and strong. The surface subsidence induced by mining will cause damage to buildings. It is assumed that the mining area is a rectangular area of 500 m × 300 m. According to the “Rules for the mine extraction and coal pillars establishment under buildings, water bodies, railways and main laneways” (China National Bureau of Coal Industry 2017), the protection index of the buildings and structures is determined as follows: the tilt deformation value is not more than 3.0 mm/m, the horizontal deformation value is not more than 2.0 mm/m, and the curvature deformation value is not more than 0.2 mm/m<sup>2</sup>. To protect the buildings, the protection index is set to the same as the above.

### Design of schemes and selection of predicted parameters

According to the monitoring data of surface movement and deformation in the mining area and the predicted parameters of the probability integral method in the mining area with similar geological conditions, the predicted parameters of the probability integral method of the caving mining in the study area are determined, as shown in Table 4.

Five mining schemes have been designed in the study area:

- Scheme 1 adopts the backfill mining method with a filling rate of 80% and the equivalent mining height of 0.4 m.
- Scheme 2 adopts the backfill mining method with a filling rate of 85% and the equivalent mining height of 0.3 m.
- Scheme 3 adopts the backfill-strip mining method with a filling rate of 85%, the width of the caving mining work-

**Table 4** Predicted parameters of the probability integral method of the caving mining in the study area

Subsidence coefficient ( $q$ )	Horizontal movement coefficient ( $b_0$ )	Tangent of major influence angle ( $\tan\beta$ )	Propagation angle of extraction ( $\theta_0$ )	Inflection point offset ( $S$ )
0.6	0.3	1.6	90°-0.8 $\alpha$	0.18H

ing face of 30 m and the width of the backfill working face of 40 m.

Scheme 4 adopts the backfill-strip mining method with a filling rate of 85%, the width of the caving mining working face of 40 m and the width of the backfill working face of 40 m.

Scheme 5 adopts the backfill-strip mining method with a filling rate of 85%, the width of the caving mining working face of 50 m and the width of the backfill working face of 40 m.

According to the superposition calculation method of the backfill-strip mining in “Study of the numerical simulation experiment,” the predicted parameters of the probability integral method in five schemes are determined. The surface subsidence prediction of the backfill mining is based on the equivalent mining height theory (Miao et al. 2010; Guo et al. 2014). The equivalent mining height theory is to calculate the maximum surface subsidence value by replacing the actual mining height of the coal seam with the calculated equivalent mining height. The calculation equation is  $W_0 = m_e q_e \cos\alpha$ , where  $m_e$  is the equivalent mining height;  $q_e$  is the subsidence coefficient of the backfill mining. The subsidence coefficient of the backfill mining based on equivalent mining height theory is approximately equal to that of the caving mining. The tangent of major influence angle is 0.2~0.5 smaller than that of the caving mining. The horizontal movement coefficient and propagation angle of extraction are the same as those of the caving mining. The predicted parameters of each scheme are shown in Table 5.

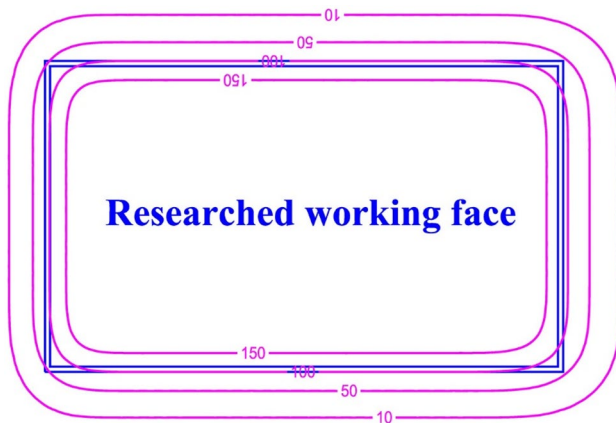
### Analysis of scheme result

For the above five schemes, the mining subsidence prediction and analysis system based on the principle of the probability integral method is used to predict the mining subsidence of each scheme. The surface movement and deformation values of each scheme are calculated. Due to space limitations, only the surface subsidence contour map of scheme 3 is drawn, as shown in Fig. 12.

According to the contour map of surface movement and deformation, the extreme values of surface movement and deformation of each scheme are statistically obtained as shown in Table 6. Because the curvature deformation of each

**Table 5** Prediction parameters of probability integral method for different mining schemes in the study area

Scheme	Subsidence coefficient ( $q$ )	Horizontal movement coefficient ( $b_0$ )	Tangent of major influence angle ( $\tan\beta$ )	Propagation angle of extraction ( $\theta_0$ )	Inflection point offset ( $S$ )
Scheme 1	0.6	0.3	1.4	$90^\circ-0.8\alpha$	0
Scheme 2	0.6	0.3	1.4	$90^\circ-0.8\alpha$	0
Scheme 3	0.18	0.25	1.5	$90^\circ-0.8\alpha$	0
Scheme 4	0.20	0.25	1.5	$90^\circ-0.8\alpha$	0
Scheme 5	0.22	0.25	1.5	$90^\circ-0.8\alpha$	0

**Fig. 12** Surface subsidence contour map of scheme 3**Table 6** Extreme value of surface movement and deformation for each scheme

Scheme	Maximum subsidence (mm)	Tilt (mm/m)	Horizontal movement (mm)	Horizontal deformation (mm/m)
Scheme 1	240	3.6	64	1.4
Scheme 2	180	2.6	48	1.0
Scheme 3	200	3.0	54	1.2
Scheme 4	240	3.6	64	1.4
Scheme 5	280	4.2	75	1.6

scheme is very small, it is within the range of the protection index, and no statistics are made here.

As shown in Table 6, the filling rate is inversely proportional to the surface movement and deformation when the backfill mining is adopted. When the filling rate is set to 85%, the maximum surface subsidence value, the extreme tilt value, and the extreme horizontal deformation value are 180 mm, 2.6 mm/m, and 1.0 mm/m, respectively, which are within the range of protection index of the mining area. When backfill-strip mining is adopted with a filling rate of 85%, the width of the caving face is proportional to the surface movement and deformation. When the width of the caving mining working face increases from 30 to 50 m, the

maximum subsidence value of the surface increases from 200 to 280 mm, the extreme value of tilt increases from 3.0 to 4.2 mm/m, and the extreme value of horizontal deformation increases from 1.2 to 1.6 mm/m. When the width of the caving mining working face is 30 m, the surface movement and deformation value is within the range of the protection index. Compared with scheme 2, scheme 3 cannot only protect ground buildings but also reduce the input of filling materials, save mining costs, and increase the economic benefits. Analyzing synthetically, scheme 3 is the best mining scheme.

## Conclusion

- (1) The characteristics of surface movement and deformation with different widths of the caving mining working face and different filling rates in the backfill-strip mining are studied by numerical simulation. It is concluded that when the width of the caving mining working face is in the range of 30~80 m, the maximum surface subsidence and the bearing stress of the filling body are directly proportional to the width of the caving mining working face. The bearing stress of coal pillars is unchanged, and the distance from the wave band to surface conforms to the quadratic function distribution. The characteristics of surface movement and deformation conform to the probability integration prediction model.
- (2) Based on the mathematical model of the probability integral method, the superposition calculation method of the backfill-strip mining is deduced, and the calculation equation of the prediction parameters of the whole backfill-strip mining area is given.
- (3) Combined with the case, five backfill-strip mining schemes are designed. According to the ground protection index and mining economic benefits, scheme 3 is finally determined as the best mining scheme. The research results provide a reference for the prediction of surface subsidence in mining areas with similar geological conditions.

**List of symbols**  $W_0$ : The surface maximum subsidence value of full mining;  $m$ : The thickness of coal seam;  $q$ : Surface subsidence coefficient;  $\alpha$ : Dip angle of coal seam;  $r$ : Major influence radius of the strike direction;  $\rho$ : The design filling rate of the working face;  $a$ : The width of the backfill working face;  $b$ : The width of the caving mining working face;  $\lambda$ : The recovery rate of the strip mining;  $H$ : The mining depth of coal seam;  $\tan\beta$ : The tangent of major influence angle;  $b_0$ : The horizontal movement coefficient;  $S$ : The Inflection point offset;  $\theta_0$ : The propagation angle of extraction

**Funding** This work was funded by the Innovation and Demonstration Program of Geology & Mineral Resources of Shandong Province (Grant No. HJ202206) and the Major Innovation Program of Shandong Province (Grant No. 2022CXGC011403).

## Declarations

**Conflict of interest** The authors declare no competing interests.

## References

- China National Bureau of Coal Industry (2017) Rules for the mine extraction and coal pillars establishment under buildings, water bodies, railways and main laneways. China Coal Industry Press, Beijing (in Chinese)
- Deng KZ, Tan ZX, Jiang Y et al (2014) Deformation monitoring and subsidence engineering. China University of Mining and Technology Press, Xuzhou (in Chinese)
- Diao XP, Wu K, Chen RL et al (2019) Identifying the cause of abnormal building damage in mining subsidence areas using InSAR technology. *IEEE Access* 7:172296–172304
- Dong Y, Huang YC, Zhao WP et al (2018) Research on safety of backfill mining strip pillars under villages. *China Saf Sci J* 28(08):117–122 (in Chinese)
- Ghabraie B, Ren G, Barbato J et al (2017) A predictive methodology for multi-seam mining induced subsidence. *Int J Rock Mech Min Sci* 93:280–294
- Goodarzi AR, Salimi M (2015) Stabilization treatment of a dispersive clayey soil using granulated blast furnace slag and basic oxygen furnace slag. *Appl Clay Sci* 108:61–69
- Guo GL, Wang YH, Ma ZG (2004) A new method for ground subsidence control in coal mining. *J China Univ Min Technol* 33:150–153 (in Chinese)
- Guo GL, Zhu XJ, Zha JF et al (2014) Subsidence prediction method based on equivalent mining height theory for solid backfilling mining. *Trans Nonferrous Metals Soc China* 24(10):3302–3308
- Guo GL, Li HZ, Zha JF (2019) An approach to protect cultivated land from subsidence and mitigate contamination from colliery gangue heaps. *Process Saf Environ Prot* 124:336–344
- Guo KK, Guo GL, Li HZ et al (2020) Strata movement and surface subsidence prediction model of deep backfilling mining. *Energy Sources Part A: Recover Utili Environ Eff* 2020:1–15
- Guo GL, Li HZ, Zha JF et al (2023) Research status and countermeasures of coordinated development of coal mining and cultivated land protection in the plain coal-cropland over-lapped areas. *Coal Sci Technol* 51(01):416–426 (in Chinese)
- He H, Dou LM, Fan J et al (2012) Deep-hole directional fracturing of thick hard roof for rockburst prevention. *Tunn Undergr Space Technol* 32:34–43
- He J, Dou LM, Mu ZL et al (2016) Numerical simulation study on hard-thick roof inducing rock burst in coal mine. *J Cent South Univ* 23(9):2314–2320
- Jahandari S, Tao Z, Saberian M et al (2022) Geotechnical properties of lime-geogrid improved clayey subgrade under various moisture conditions. *Road Materials and Pavement Design* 23(9):2057–2075
- Jiang Q, Guo GL, Li HZ et al (2022) Investigation of coordinated development of coal mining and pipeline protection under boundary effect of thick unconsolidated layer. *Bull Eng Geol Env* 81(4):1–12
- Khajeh A, Jamshidi Chenari R, Payan M (2020) A simple review of cemented non-conventional materials: soil composites. *Geotech Geol Eng* 38(2):1019–1040
- Khajeh A, Ebrahimi SA, MolaAbasi H, Jamshidi Chenari R, Payan M (2021) Effect of EPS beads in lightening a typical zeolite and cement-treated sand. *Bull Eng Geol Env* 80(11):8615–8632
- Khajeh A, Jamshidi Chenari R, MolaAbasi H, Payan M (2022) An experimental investigation on geotechnical properties of a clayey soil stabilised with lime and zeolite in base and subbase courses. *Road Mater Pavement Des* 23(12):2924–2941
- Khaksar Najafi E, Jamshidi Chenari R, Payan M, Arabani M (2021) A sustainable landfill liner material: clay-fly ash geopolymers. *Bull Eng Geol Env* 80(5):4111–4124
- Khanal M, Hodgkinson JH (2021) Subsidence prediction versus observation in Australia: a short comment. *Environ Impact Assess Rev* 86:106479
- Li HZ, Guo GL, Zhai SC (2016) Mining scheme design for super-high water backfill strip mining under buildings: a Chinese case study. *Environ Earth Sci* 75(12):1–12
- Li HZ, Zha JF, Guo GL (2019) A new dynamic prediction method for surface subsidence based on numerical model parameter sensitivity. *J Clean Prod* 233:1418–1424
- Li M, Zhang JX, Sun K et al (2019) Reducing surface subsidence risk using solid waste backfill technique: a case study under buildings. *Polish Journal of Environmental Studies* 28(5):3333–3341
- Miao XX, Zhang JX, Guo GL (2010) Study on waste-filling method and technology in fully-mechanized coal mining. *J China Coal Soc* 35(01):1–6 (in Chinese)
- Ngamkhanong C, Keawsawasvong S, Jearsiripongkul T, Cabangon LT, Payan M, Sangjinda K, ..., Thongchom C (2022) Data-driven prediction of stability of rock tunnel heading: an application of machine learning models. *Infrastructures* 7(11):148
- Nie L, Zhang M, Jian HQ (2013) Analysis of surface subsidence mechanism and regularity under the influence of seism and fault. *Nat Hazards* 66(2):773–780
- Saeidi A, Deck O, Verdel T (2012) Development of building vulnerability functions in subsidence regions from analytical methods. *Geotechnique* 62(2):107–120
- Salmi EF, Nazem M, Karakus M (2017) Numerical analysis of a large landslide induced by coal mining subsidence. *Eng Geol* 217:141–152
- Senol A (2012) Effect of fly ash and polypropylene fibres content on the soft soils. *Bull Eng Geol Env* 71(2):379–387
- Shirmohammadi S, Ghaffarpour Jahromi S, Payan M, Senetakis K (2021) Effect of lime stabilization and partial clinoptilolite zeolite replacement on the behavior of a silt-sized low-plasticity soil subjected to freezing–thawing cycles. *Coatings* 11(8):994
- Tan YL, Zhang Z, Zhao TB (2011) AE pattern of rock burst disaster induced by strata activation in coal mine. *Disaster Adv* 12(4):29–33
- Venik G, Bang-Kittilsen A, Boogaard FC (2020) Risk assessment for areas prone to flooding and subsidence: a case study from Bergen, Western Norway. *Hydrol Res* 51(2):322–338
- Vusovic N, Vlahovic M, Krzanovic D (2021) Stochastic method for prediction of subsidence due to the underground coal mining integrated with GIS, a case study in Serbia. *Environ Earth Sci* 80(2):1–29
- Wang ZS, Deng KZ (2012) Edge-amended model of probability-integral method for subsidence prediction. *J Xian Univ Sci Technol* 32(04):495–499 (in Chinese)

- Wang QC, Guo GL (2020) Analysis of surface subsidence and deformation of thick mechanized coal gangue filling mining under village. *Saf Coal Min* 51(1):222–228 (in Chinese)
- Wang F, Miao L (2009) A proposed lightweight fill for embankments using cement-treated Yangzi River sand and expanded polystyrene (EPS) beads. *Bull Eng Geol Env* 68(4):517–524
- Wang L, Li N, Zhang XN (2015) Surface subsidence quantitative control method of shallow buried coal mining with strip mining solid backfilling. *Saf Coal Min* 46(11):31–34 (in Chinese)
- Wang W, Cheng YP, Wang HF et al (2015b) Coupled disaster-causing mechanisms of strata pressure behavior and abnormal gas emissions in underground coal extraction. *Environ Earth Sci* 74(9):6717–6735
- Wang H-S, Tang C-S, Gu K, Shi B, Inyang HI (2020) Mechanical behavior of fiber-reinforced, chemically stabilized dredged sludge. *Bull Eng Geol Env* 79(2):629–643
- Wei T, Guo GL, Li HZ et al (2022) Fusing minimal unit probability integration method and optimized quantum annealing for spatial location of coal goafs. *KSCE J Civ Eng* 26(5):2381–2391
- Xuan DY, Xu JL (2014) Grout injection into bed separation to control surface subsidence during longwall mining under villages: case study of Liudian coal mine, China. *Nat Hazards* 73(2):883–906
- Yuan YF, Li HZ, Zhang HJ et al (2020) Improving reliability of prediction results of mine surface subsidence of Northern Pei County for reusing land resources. *Appl Sci* 10(23):8385
- Zha JF, Guo GL, Feng WK et al (2011) Mining subsidence control by solid backfilling under buildings. *Trans Nonferrous Metals Soc China* 21:670–674
- Zhang JX, Zhang Q, Sun Q et al (2015) Surface subsidence control theory and application to backfill coal mining technology. *Environ Earth Sci* 74(2):1439–1448
- Zhang Q, Liu H, Zhai SC et al (2017) Design and effect evaluation of the filling strip mining scheme under buildings. *Metal Mine* 496(10):105–109 (in Chinese)
- Zhou N, Liu HF, Zhang JX et al (2019) Study on rock burst event disaster and prevention mechanisms of hard roof. *Adv Civ Eng* 2019:1–14
- Zhu XJ, Guo GL, Zha JF et al (2016) Surface dynamic subsidence prediction model of solid backfill mining. *Environ Earth Sci* 75(12):1–9
- Zhu XJ, Guo GL, Liu HZ et al (2019a) Experimental research on strata movement characteristics of backfill-strip mining using similar material modeling. *Bull Eng Geol Env* 78(4):2151–2167
- Zhu XJ, Guo GL, Liu HZ et al (2019b) Surface subsidence prediction method of backfill-strip mining in coal mining. *Bull Eng Geol Env* 78(8):6235–6248
- Zhu XJ, Zha F, Guo GL et al (2021) Subsidence control design method and application to backfill-strip mining technology. *Adv Civ Eng* 2021:1–15

Springer Nature or its licensor (e.g. a society or other partner) holds exclusive rights to this article under a publishing agreement with the author(s) or other rightsholder(s); author self-archiving of the accepted manuscript version of this article is solely governed by the terms of such publishing agreement and applicable law.